ISSN 0027-1314, Moscow University Chemistry Bulletin, 2008, Vol. 63, No. 4, pp. 207–213. © Allerton Press, Inc., 2008.
Original Russian Text © K.V. Oskolok, O.V. Monogarova, 2008, published in Vestnik Moskovskogo Universiteta. Khimiya, 2008, No. 4, pp. 252–259.

Excitation of X-ray Fluorescence of Thin-Film Samples by Bremsstrahlung: Extension and Analytical Possibilities of the Monochromatic Model

K. V. Oskolok and O. V. Monogarova

Department of Analytical Chemistry
e-mail: oskolok@analyt.chem.msu.ru

Received March 19, 2007

Abstract—Different approaches to the description of X-ray fluorescence excitation in thin films by bremsstrahlung within the monochromatic model are systematically expounded and compared. New analytical expressions are proposed for calculation of the wavelength of a virtual monochromatic excitation source. It is shown that some of them can be successfully used in quantitative X-ray fluorescence analysis of semiinfinite samples, including matrix effects, without a priori information on an analyte.

DOI: 10.3103/S0027131408040081

An important problem of quantitative X-ray fluorescence (XRF) analysis of complex multielement systems is correct consideration of matrix effects, among which is the effect of filtration of the polychromatic emission spectrum of an X-ray tube by the surface layers of an analyte. Due to a strong dependence of the absorption coefficient on the X-ray radiation wavelength and the nature and contents of analytes and matrix components, XRF of deep-seated layers of the sample is excited by primary radiation of a significantly different composition. In addition to the polychromatic approach, the monochromatic approximation is used for describing this process. The continuous wave distribution of X-ray tube emission is replaced by the δ-function of a virtual monochromatic source (VMS) of radiation with an analogous excitation effect [1–4]. The VMS parameters found are used for calculating correction factors for matrix effects in quantitative XRF analysis by the internal or external reference method or the fundamental parameter method. This approach is elegant, has a clear physical meaning, and implies a noticeably smaller amount of computations, but leads to a higher error of analysis [5]. However, for any wavelength of the polychromatic emission spectrum of an X-ray tube, the error of determination of the XRF excitation efficiency is limited, first of all, by the degree of uncertainty of the fundamental parameters used. Under these conditions, the monochromatic model can ensure a comparable error of XRF analysis if the VMS wavelength is properly selected [6]. Therefore, the VMS parameters calculated by approximate analytical expressions should be corrected for the elemental composition of a sample and the special design features of the X-ray tube used.

For massive XRF emitters, the VMS parameters of primary radiation are determined by the X-ray tube characteristics, the spectrometer geometry, and the a priori unknown composition of an analyte. The error of the analysis results depends very strongly on the choice of the VMS wavelength. The smallest error is ensured by the use of the so-called analytical equivalent wavelength (AEWL) (found empirically), which depends only slightly on the analyte concentration [4]. When XRF is excited in thin films, the effect of filtration of polychromatic X-ray tube radiation is not pronounced. For very thin XRF emitters, the VMS parameters depend on the X-ray tube emission spectrum and the nature of the analyte element but are not related to its content [7–9]. Therefore, the error of analysis results for thin films is almost independent of the chosen VMS wavelength. However, with a change in the conditions of measurement of the analytical signal, the VMS parameters calculated by a given algorithm for massive and thin-film samples change nearly in parallel. It is of special practical interest to find a simple analytical expression for calculation of the VMS wavelength of XRF excitation in a thin-film emitter close to the AEWL for a semiinfinite sample studied on a spectrometer with a given geometry. The use of such an algorithm is quite instructive in quantitative XRF analysis of complex (including unique) analytes without a priori information on their compositions and properties when preparation of reference samples is too laborious a task.

The aim of this study is to compare the analytical possibilities of different algorithms for the description of the process of XRF excitation in thin films by bremsstrahlung within the monochromatic model taking into account the nature of the analyte element and the design features of an X-ray tube.

THEORY

The XRF intensity of the *i*th element excited in a thin film by X-ray tube radiation can be calculated by Sherman or Blokhin equation

$$I_i = C_i \omega_i f_i \frac{S_{q2} - 1}{S_{q2}} \rho d \int_{\lambda_0}^{\lambda_{q2}} \Phi(\lambda) d\lambda, \quad (1)$$

where C_i is the content of the *i*th element; ω_i is the $q2$ fluorescence yield of the *i*th element; f_i is the contribution of the analytical line to the total intensity of the $q2$ series; λ_{q2} and S_{q2} are the wavelength and jump of the $q2$-edge of absorption of the *i*th element, respectively; λ_0 is the short-wave edge of the bremsstrahlung spectrum; ρ and d are the density and thickness of the analyte sample. The integrand is

$$\Phi_{\text{Sherman}}(\lambda) = \tau_i(\lambda) I_0(\lambda), \quad (2)$$

$$\Phi_{\text{Blokhin}}(\lambda) = \tau_i(\lambda) I_0(\lambda) \lambda / \lambda_i, \quad (3)$$

where I_0 is the primary radiation intensity; τ_i is the mass absorption coefficient of the *i*th element for primary radiation; and λ and λ_i are the wavelengths of primary and fluorescence radiation, respectively [10, 11]. Thus, the Sherman (or Blokhin) equation allows one to determine the number of XRF quanta (or the energy) emitted by the sample surface per excitation quantum (or per unit energy of primary radiation).

As a first approximation, the wave distribution of the bremsstrahlung intensity of the X-ray tube can be described by the Kramers equation:

$$I_0(\lambda) = k_1 Z_{\text{an}} j (\lambda - \lambda_0) / \lambda_0 \lambda^3, \quad (4)$$

where k_1 is a constant, Z_{an} is the atomic number of the anode material of the X-ray tube, and j is the current density [1]. The mass absorption coefficients (cm^2/g) in a wide range of wavelengths (Å) can be estimated by the formula

$$\tau_i(\lambda) \approx 0.016 Z_i^{3.94} \lambda^3 / A_i \prod_{r=1}^{m} S_{q_r}, \quad (5)$$

where Z_i and A_i are the atomic number and atomic weight of the *i*th element, respectively; and m is the number of absorption jumps (S_q) on the wavelength interval $[0, \lambda]$. However, for more accurate calculations of the power function of wavelength, the floating exponent t should be introduced depending on the chemical element to be determined [12]:

$$\tau_i(\lambda) = k_2(Z_i, \lambda) \lambda^t, \quad t \in [2.5; 4], \quad (6)$$

where k_2 is the constant for the corresponding element in wavelength ranges between absorption edges. To calculate the VMS wavelength, we used the first mean-value theorem for the function $\Phi(\lambda)$ on the wavelength interval $[\lambda_1, \lambda_2]$ provided that it is continuous (algorithm 1),

$$\int_{\lambda_1}^{\lambda_2} \Phi(\lambda) d\lambda = \overline{\Phi(\lambda)} (\lambda_2 - \lambda_1) \quad (7)$$

and the second (generalized) mean-value theorem (algorithm 2),

$$\int_{\lambda_1}^{\lambda_2} \Phi(\lambda) d\lambda = \bar{\lambda} \int_{\lambda_1}^{\lambda_2} (\Phi(\lambda)/\lambda) d\lambda. \quad (8)$$

In algorithm 3, a procedure of averaging over the argument values $\bar{\lambda}$ was used assuming that the weighting function $\Phi(\lambda)$ on the wavelength interval $[\lambda_1, \lambda_2]$ is continuous:

$$\int_{\lambda_1}^{\tilde{\lambda}} \Phi(\lambda) d\lambda = \int_{\tilde{\lambda}}^{\lambda_2} \Phi(\lambda) d\lambda. \quad (9)$$

A more correct wave distribution of the bremsstrahlung intensity of the X-ray tube can be calculated by the formula [13]

$$I_0(\lambda) = k_3 Z_{\text{an}} \frac{\lambda - \lambda_0}{\lambda_0^{1+a} \lambda^{2-a}} \times \ln^{-1}\left(\frac{1166(2E_0 + E_\lambda)}{3J}\right) R_\lambda f_\lambda \exp(-\mu_\lambda^{\text{Be}} \rho_{\text{Be}} d_{\text{Be}}), \quad (10)$$

where k_3 is a constant; a is a parameter depending on Z_{an}; E_0 and E_λ are the electron and bremsstrahlung photon energies (keV), respectively; $J = 11.5 Z_{\text{an}}$ is the average ionization potential of anode atoms (eV); R is the backscattering factor of electrons in the anode [14]; μ^{Be} is the mass attenuation coefficient of the Be window; ρ_{Be} id the beryllium density; and d_{Be} is the Be window thickness. The Philibert absorption correction (mass coefficient μ^{an}) is

$$f_\lambda = (1 + \mu_\lambda^{\text{an}} \sigma_\lambda^{-1} \sin^{-1}\psi)^{-1} (1 + h \mu_\lambda^{\text{an}} \sigma_\lambda^{-1} \sin^{-1}\psi)^{-1} \quad (11)$$

Table 1. Formulas for calculation of the VMS wavelength obtained on the basis of the Sherman equation*

No. of equation	Condition	Equation
		Algorithm 1
(1.1.1)	$\forall t \in [2.5; 4]$	$\bar{\lambda}^{t-2} - \lambda_0\bar{\lambda}^{t-3} = \frac{\lambda_u^{t-1} - \lambda_l^{t-1}}{(t-1)(\lambda_u - \lambda_l)} - \frac{\lambda_0(\lambda_u^{t-2} - \lambda_l^{t-2})}{(t-2)(\lambda_u - \lambda_l)}$
(1.1.2)	$t = 3$, $\lambda_l = \lambda_0$, $\lambda_u = \lambda_{q2}$	$\bar{\lambda} = (\lambda_0 + \lambda_{q2})/2$
(1.1.3)	$t = 3$, $\lambda_l = \lambda_{q1}$, $\lambda_u = \lambda_{q2}$	$\bar{\lambda} = (\lambda_{q1} + \lambda_{q2})/2$
		Algorithm 2
(1.2.1)	$t \in [2.5; 4]$, $t \neq 3$	$\bar{\lambda} = \frac{t-3}{t-1}\frac{(t-2)(\lambda_u^{t-1} - \lambda_l^{t-1}) - (t-1)\lambda_0(\lambda_u^{t-2} - \lambda_l^{t-2})}{(t-3)(\lambda_u^{t-2} - \lambda_l^{t-2}) - (t-2)\lambda_0(\lambda_u^{t-3} - \lambda_l^{t-3})}$
(1.2.2)	$t = 3$, $\lambda_l = \lambda_0$, $\lambda_u = \lambda_{q2}$	$\bar{\lambda} = \frac{1}{2}\frac{(\lambda_{q2} - \lambda_0)^2}{\lambda_{q2} - \lambda_0(1 + \ln\lambda_{q2}/\lambda_0)}$
(1.2.3)	$t = 3$, $\lambda_l = \lambda_{q1}$, $\lambda_u = \lambda_{q2}$	$\bar{\lambda} = \frac{(\lambda_{q2} - \lambda_{q1})(\lambda_{q2} + \lambda_{q1} - 2\lambda_0)}{2(\lambda_{q2} - \lambda_{q1} - \lambda_0\ln\lambda_{q2}/\lambda_{q1})}$
		Algorithm 3
(1.3.1)	$\forall t \in [2.5; 4]$	$\frac{2\tilde{\lambda}^{t-1}}{t-1} - \frac{2\lambda_0\tilde{\lambda}^{t-2}}{t-2} = \frac{\lambda_u^{t-1} + \lambda_l^{t-1}}{t-1} - \frac{\lambda_0(\lambda_u^{t-2} + \lambda_l^{t-2})}{t-2}$
(1.3.2)	$t = 3$, $\lambda_l = \lambda_0$, $\lambda_u = \lambda_{q2}$	$\tilde{\lambda} = \lambda_0 + \frac{\lambda_{q2} - \lambda_0}{\sqrt{2}}$
(1.3.3)	$t = 3$, $\lambda_l = \lambda_{q1}$, $\lambda_u = \lambda_{q2}$	$\tilde{\lambda} = \lambda_0 + \sqrt{\frac{(\lambda_{q1} - \lambda_0)^2 + (\lambda_{q2} - \lambda_0)^2}{2}}$

* See text for details.

in a massive anode and

$$f_\lambda = \frac{\exp(-\mu_\lambda^{an}\rho_{an}d_{an})(1-h) - \exp(-\sigma_\lambda\rho_{an}d_{an})}{(1-\mu_\lambda^{an}/\sigma_\lambda)(1-h-\exp(-\sigma_\lambda\rho_{an}d_{an}))}, \quad h = \frac{1.2A_{an}/Z_{an}^2}{1+1.2A_{an}/Z_{an}^2} \tag{12}$$

in a thin-film anode. Here, ψ is the take-off angle of anode radiation; A_{an}, ρ_{an}, and d_{an} are the atomic weight, density, and thickness of the anode; and σ is the electron energy loss factor

$$\sigma = 4 \times 10^5/(E_0^{1.65} - E_\lambda^{1.65}). \tag{13}$$

This procedure was used in this work for numerical calculation of the VMS wavelength corrected for the design features of the X-ray tube.

EXPERIMENTAL

To study the possibility of using the suggested algorithms for calculation of the VMS wavelength in quantitative analysis of massive objects, we determined the contents of Zn and Ni in certified specimens of aluminum alloy and steel (metallic cylinders ∅ 12 × 4 mm in size with a polished surface) by the external reference method with corrections for absorption. The spectra were measured on a Spektron Spectroscan-G Max series XRF spectrometer (Russia) equipped with a low-power (4 W) sharp-focus (∅ 1.5 mm) end-window X-ray tube with a thin-film (2 μm) Cr anode. The thickness of the Be window was 200 μm. The working voltage and current were 40 kV and 100 μA, respectively. The angle of incidence of primary radiation was 80° and the take-off angle of secondary radiation was 30°. A LiF (200) crystal analyzer ($2d$ = 4028 mÅ) was used

Table 2. Formulas for calculation of the VMS wavelength obtained on the basis of the Blokhin equation*

No. of equation	Condition	Equation
		Algorithm 1
(2.1.1)	$\forall t \in [2.5; 4]$	$\bar{\lambda}^{t-1} - \lambda_0\bar{\lambda}^{t-2} = \frac{\lambda_u^t - \lambda_l^t}{t(\lambda_u - \lambda_l)} - \frac{\lambda_0(\lambda_u^{t-1} - \lambda_l^{t-1})}{(t-1)(\lambda_u - \lambda_l)}$
(2.1.2)	$t = 3$, $\lambda_l = \lambda_0$, $\lambda_u = \lambda_{q2}$	$\bar{\lambda} = \frac{\lambda_0}{2} + \frac{\lambda_{q2}}{2}\sqrt{1 + \frac{1}{3}\left(1 - \frac{\lambda_0}{\lambda_{q2}}\right)^2}$ [7]
(2.1.3)	$t = 3$, $\lambda_l = \lambda_{q1}$, $\lambda_u = \lambda_{q2}$	$\bar{\lambda} = \frac{\lambda_0}{2} + \sqrt{\frac{\lambda_0^2}{4} - \frac{\lambda_0(\lambda_{q1} + \lambda_{q2})}{2} - \frac{\lambda_{q1}\lambda_{q2} - (\lambda_{q1} + \lambda_{q2})^2}{3}}$
		Algorithm 2
(2.2.1)	$\forall t \in [2.5; 4]$	$\bar{\lambda} = \frac{t-2}{t}\frac{(t-1)(\lambda_u^t - \lambda_l^t) - t\lambda_0(\lambda_u^{t-1} - \lambda_l^{t-1})}{(t-2)(\lambda_u^{t-1} - \lambda_l^{t-1}) - (t-1)\lambda_0(\lambda_u^{t-2} - \lambda_l^{t-2})}$
(2.2.2)	$t = 3$, $\lambda_l = \lambda_0$, $\lambda_u = \lambda_{q2}$	$\bar{\lambda} = \frac{2\lambda_{q2}^2 - \lambda_{q2}\lambda_0 - \lambda_0^2}{3(\lambda_{q2} - \lambda_0)}$
(2.2.3)	$t = 3$, $\lambda_l = \lambda_{q1}$, $\lambda_u = \lambda_{q2}$	$\bar{\lambda} = \frac{2(\lambda_{q1}^2 + \lambda_{q1}\lambda_{q2} + \lambda_{q2}^2) - 3\lambda_0(\lambda_{q1} + \lambda_{q2})}{3(\lambda_{q1} + \lambda_{q2} - 2\lambda_0)}$
		Algorithm 3
(2.3.1)	$\forall t \in [2.5; 4]$	$\frac{2\tilde{\lambda}^t}{t} - \frac{2\lambda_0\tilde{\lambda}^{t-1}}{t-1} = \frac{\lambda_u^t + \lambda_l^t}{t} - \frac{\lambda_0(\lambda_u^{t-1} + \lambda_l^{t-1})}{t-1}$
(2.3.2)	$t = 3$, $\lambda_l = \lambda_0$, $\lambda_u = \lambda_{q2}$	$\tilde{\lambda} = b + \frac{(a + \sqrt{a^2 - b^6})^{2/3} + b^2}{(a + \sqrt{a^2 - b^6})^{1/3}}$; $a = \frac{2\lambda_{q2}^3 - 3\lambda_0\lambda_{q2}^2}{8}$; $b = \frac{\lambda_0}{2}$
(2.3.3)	$t = 3$, $\lambda_l = \lambda_{q1}$, $\lambda_u = \lambda_{q2}$	See Eq. (2.3.2) at $a = (2\lambda_{q1}^3 + 2\lambda_{q2}^3 - \lambda_0^3 - 3\lambda_0\lambda_{q1}^2 + 3\lambda_0\lambda_{q2}^2)/8$

* See text for details.

for converting secondary radiation to a wave spectrum by the Johansson method. For detection of secondary X-ray quanta, the spectrometer was equipped with a sealed gas-discharge proportional counter. The contents of Zn and Ni were determined from the ZnK_β (1295 mÅ) and NiK_β (1500 mÅ) line intensities. The exposure time was 10 s (the counting rate was above 5000 counts/s). Corrected spectral line intensities were found by measuring the amplitude distribution of the XRF intensity of the analyte element with a step of 2 mÅ and the continuous spectral component in the vicinity of the characteristic peak (±50 mÅ) followed by correction of the background signal.

RESULTS AND DISCUSSION

Tables 1 and 2 lists general formulas for calculation of the VMS wavelength of XRF excitation in thin films with floating parameters (Eqs. (x.x.1)) for the entire interval of bremsstrahlung wavelengths from the short-wave edge λ_0 to the absorption edge λ_{q2} of the analyte element (Eqs. (x.x.2)), as well for an arbitrary interval, for example, between the absorption edges of the interfering and analyte elements (λ_{q1}, λ_{q2}) (Eqs. (x.x.3)). In XRF analysis of very thin samples with the use of characteristic K lines, the VMS parameters can be calculated by Eqs. (x.x.2): matrix effects are negligible. When emitters of finite thickness and high density are

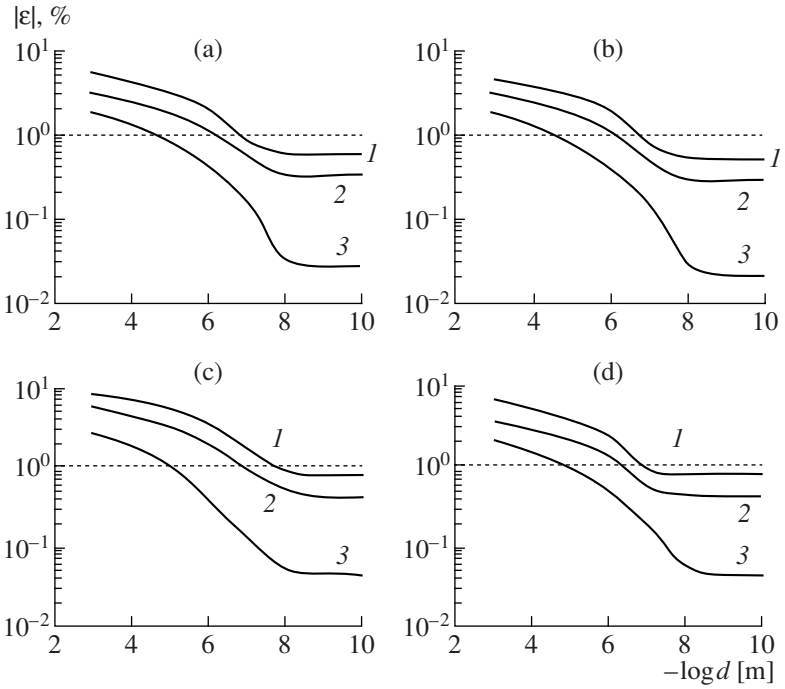

Fig. 1. Theoretical dependence of the error of determination for (a, b) 1 and (c, d) 50 wt % Fe in (a, c) a Fe–Cr alloy and (b, d) an oxide matrix on the thickness of a sample obtained with the use of different algorithms for calculation of the VMS wavelength: (*1*) Eq. (1.1.2), (*2*) Eq. (1.2.2), and (*3*) Eq. (1.3.2). The anode voltage of the X-ray tube is 45 kV, the angle of incidence of primary radiation is 35°, and the take-off angle of secondary radiation was 55°.

used in the presence of interfering elements ($\lambda_0 < \lambda_{q1} < \lambda_{q2}$), as well as when characteristic L lines are used (if $\lambda_0 < \lambda_K$), $m + 1$ VMSs should be introduced (Eqs. (x.x.3)), where m is the number of absorption jumps on the wavelength interval $[\lambda_0, \lambda_{q2}]$.

Figure 1 shows the plots of the theoretical error of quantitative XRF analysis with corrections for absorption versus the thickness of a thin-film sample obtained with the use of different algorithms of calculation of the VMS wavelength. The smallest error is achieved when Eq. (1.3.2) is used. The use of Eqs. (1.2.2) and (1.1.2) leads to a two- to fourfold increase in the error. For thin-film samples with a density up to 8–10 g/cm^3 (ores, minerals, some metal alloys), a 1% level of the relative error of XRF analysis results persists at a thickness of no more than 10–15 μm and a 2% level, up to a thickness of 1 mm (Fig. 1).

Generally, there is a simple relationship between approximate VMS wavelengths calculated by algorithm nos. 1–3 and the corresponding exact values found numerically for real X-ray tubes, which is approximated by a parabolic function with a correlation coefficient no less than 0.98. An example of such a relationship is shown in Fig. 2. The same relationship is valid when the anode material (Cr, Mo, W) and thickness (from 2 μm to ∞) and the Be window thickness (75–300 μm) are varied simultaneously. When only one experimental parameter—the atomic number of the analyte element (Z = 11–50) or the working voltage on the electrodes of the X-ray tube (20–60 kV)—is changed, the relationship between the given VMS wavelengths becomes linear. Thus, the procedure of correction of approximate VMS wavelengths taking into account the specific features of the wave distribution of the bremsstrahlung intensity of the X-ray tube

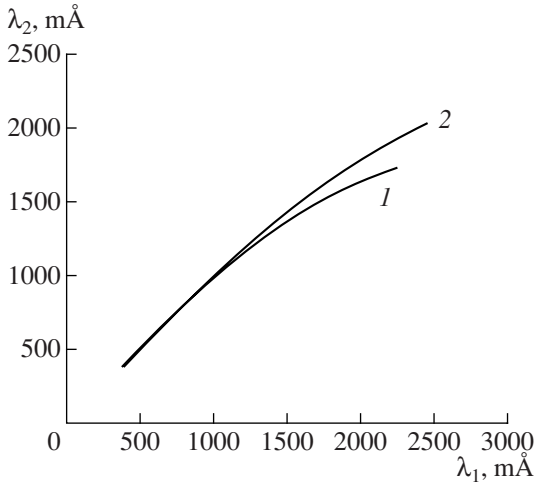

Fig. 2. Correlation between approximate (λ_1) and exact (λ_2) VMS wavelengths calculated with the use of (*1*) Eq. (1.3.2) and (*2*) Eq. (2.3.2) for an end-window X-ray tube with a thin-film (2 μm) anode.

Table 3. Relative error (%) of the quantitative XRF analysis results of certified metal alloys obtained with the use of different algorithms for calculation of VMS parameters ($f = 4$, $p = 0.95$)

Algorithm	Determination of 6.72 wt % Ni in steel		Determination of 8.87 wt % Zn in duralumin	
	calculation of XRF intensity			
	according to Blokhin	according to Sherman	according to Blokhin	according to Sherman
[1]	4.3	4.6	3.5	3.8
[2]	3.3	5.6	2.9	4.1
[3]	3.0	3.7	2.5	3.1
[4]	2.6	1.3	1.4	1.4
(1.1.2)	4.8	3.6	3.8	3.7
(1.2.2)	3.2	1.9	2.4	1.4
(1.3.2)	1.0	1.2	1.0	1.1
(2.1.2)	3.4	2.5	3.1	2.0
(2.2.2)	1.5	1.1	1.3	1.0
(2.3.2)	2.3	2.9	1.9	1.6

with a thin-film or massive anode presents no special problem.

The smallest error of the results of quantitative XRF analysis of semiinfinite samples corrected for matrix effects is achieved using the AEWL of the polychromatic spectrum of the X-ray tube [4, 15]. Previously [16], we described a new algorithm for calculation of the AEWL for samples of variable thickness, which

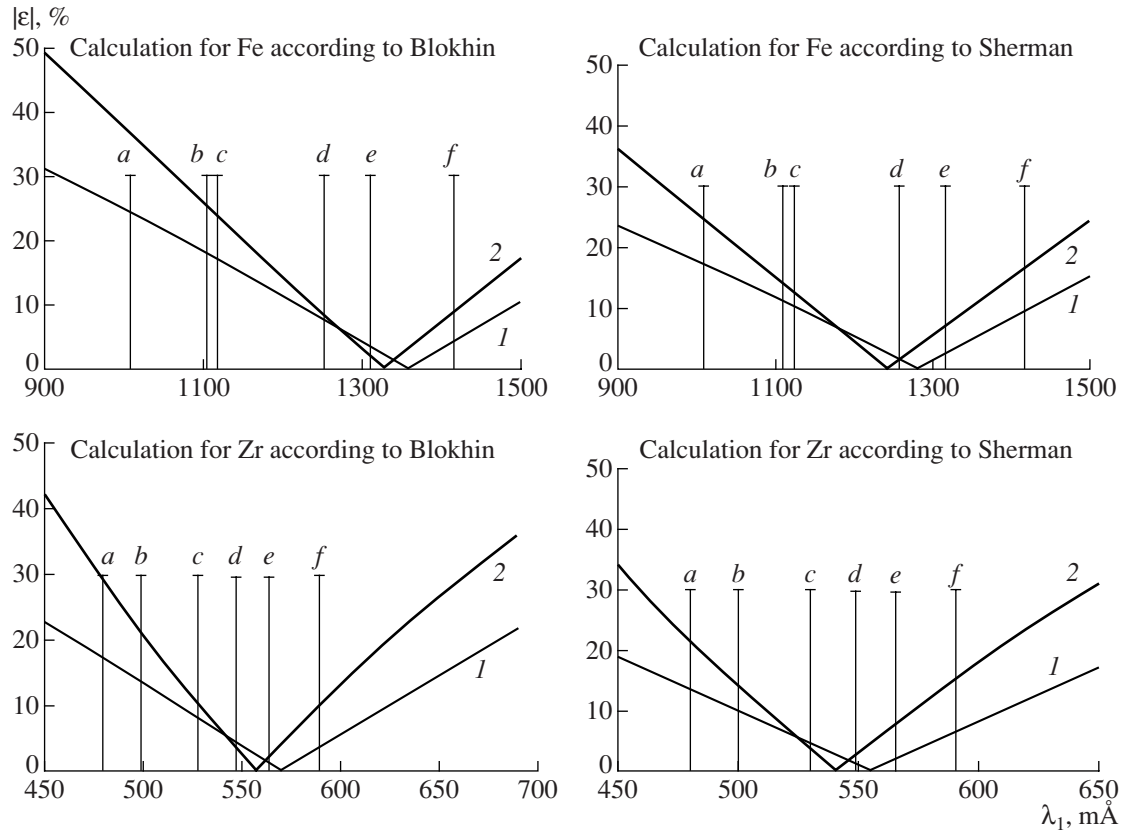

Fig. 3. Comparison of the errors of determination of (*1*) 1 and (*2*) 50 wt % iron and zirconium in a semiinfinite sample (Cr filler) obtained with the use of different algorithms for calculation of the VMS wavelength: (*a*) Eq. (1.1.2), (*b*) Eq. (2.1.2), (*c*) Eq. (1.2.2), (*d*) Eq. (2.2.2), (*e*) Eq. (1.3.2), and (*f*) Eq. (2.3.2). The anode voltage of the X-ray tube is 45 kV, the angle of incidence of primary radiation is 35°, and the take-off angle of secondary radiation was 55°.

allows for the use of thin-film references in XRF determination of the composition of massive samples. For commercial spectrometers with wave dispersion, the incidence and take-off angles are 35°–80° and 30°–55°, respectively. For such instruments, the AEWL values calculated by the new method using algorithms (1.3.2) and (2.2.2) fall within a rather narrow range. Therefore, these formulas can be efficiently used in quantitative XRF analysis of samples of arbitrary thickness, including semiinfinite ones (Table 3, Fig. 3).

REFERENCES

1. Losev, N.F., *Kolichestvennyi rentgenospektral'nyi fluorestsentnyi analiz* (Quantitative X-ray Fluorescence Analysis), Moscow, 1969.
2. Afonin, V.P., Piskunova, L.F., Gunicheva, T.N., and Lozhkin, V.I., *Zavod. Lab.*, 1976, vol. 42, no. 6, p. 670.
3. Pavlinskii, G.V. and Kitov, B.I., *Zavod. Lab.*, 1982, vol. 48, no. 4, p. 21.
4. Tertian, R., *Spectrochim. Acta B*, 1971, vol. 26, p. 26.
5. Rousseau, R.M., *Spectrochim. Acta B*, 2006, vol. 61, p. 759.
6. Kitov, B.I., *Zh. Anal. Khim.*, 2001, vol. 56, no. 2, p. 131.
7. Krasnolutskii, V.P. and Blokhina, G.E., *Zh. Anal. Khim.*, 1980, vol. 35, no. 10, p. 1898.
8. Eritenko, A.N., Tsvetyanskii, A.L., and Titarenko, A.V., *Zavod. Lab.*, 1986, vol. 52, no. 8, p. 21.
9. Tsvetyanskii, A.L. and Eritenko, A.N., *Zavod. Lab.*, 1990, vol. 56, no. 4, p. 25.
10. Sherman, J., *Spectrochim. Acta B*, 1955, vol. 7, p. 283.
11. Blokhin, M.A., *Fizika rentgenovskikh luchei* (The Physics of X-rays), Moscow, 1953.
12. Blokhin, M.A. and Shveitser, I.G., *Rentgenospektral'nyi spravochnik* (X-ray Spectral Handbook), Moscow, 1982.
13. Finkel'shtein, A.L. and Pavlova, T.O., *Zavod. Lab.*, 1996, vol. 62, no. 12, p. 16.
14. Goldstein, J.I., Newbury, D.E., Echlin, P., et al., *Scanning Electron Microscopy and X-ray Microanalysis*, New York: Plenum, 1981. Translated under the title *Rastrovaya elektronnaya mikroskopiya i rantgenovskii mikroanaliz*, Moscow, 1984.
15. Simakov, V.A., Barinskii, R.L., and Sorokin, I.V., *Zavod. Lab.*, 1986, vol. 52, no. 2, p. 30.
16. Oskolok, K.V. and Monogarova, O.V., *Vestn. Mosk. Univ., Ser. 2. Khim*., 2008, vol. 49, p. 326.